Special Issue Article

Journal of Molecular Recognition

Received: 24 May 2013, Revised: 20 August 2013, Accepted: 21 August 2013, Published online in Wiley Online Library

(wileyonlinelibrary.com) DOI: 10.1002/jmr.2313

Spot14/Mig12 heterocomplex sequesters polymerization and restrains catalytic function of human acetyl-CoA carboxylase 2†

Sungjo Park[a,b], In-Wook Hwang[a,b,c], Yu Makishima[c], Ester Perales-Clemente[a,b], Tatsuya Kato[c], Nicolas J. Niederländer[a,b], Enoch Y. Park[c] and Andre Terzic[a,b]*

Acetyl-CoA carboxylase 2 (ACC2) is an isoform of ACC functioning as a negative regulator of fatty acid β-oxidation. Spot14, a thyroid hormone responsive protein, and Mig12, a Spot14 paralog, have recently been identified as regulators of fatty acid synthesis targeting ACC1, a distinctive subtype of ACC. Here, we examined whether Spot14/Mig12 modulates ACC2. Nanoscale protein topography mapped putative protein–protein interactions between purified human Spot14/Mig12 and ACC2, validated by functional assays. Human ACC2 displayed consistent enzymatic activity, and homogeneous particle distribution was probed by atomic force microscopy. Citrate-induced polymerization and enzymatic activity of ACC2 were restrained by the addition of the recombinant Spot14/Mig12 heterocomplex but only partially by the oligo-heterocomplex, demonstrating that the heterocomplex is a designated metabolic inhibitor of human ACC2. Moreover, Spot14/Mig12 demonstrated a sequestering role preventing an initial ACC2 nucleation step during filamentous polymer formation. Thus, the Spot14/Mig12 heterocomplex controls human ACC2 polymerization and catalytic function, emerging as a previously unrecognized molecular regulator in catalytic lipid metabolism. © 2013 The Authors. *Journal of Molecular Recognition* published by John Wiley & Sons, Ltd.

Additional supporting information may be found in the online version of this article at the publisher's web site.

Keywords: Spot14; Mig12; acetyl-CoA carboxylase; protein–protein interactions; atomic force microscopy; *Thrsp*; silkworm *Bombyx mori*; fatty acid oxidation

INTRODUCTION

Lipid metabolism is vital in supporting dynamic cellular functions ensuring the balance in anabolic/catabolic homeostasis (Wakil and Abu-Elheiga, 2009; Lopaschuk *et al*., 2010; Folmes *et al*., 2013; Knobloch *et al*., 2013). Altered fatty acid metabolism precipitates a spectrum of metabolic dysfunctions including obesity, diabetes and cardiovascular disease. Central in lipid metabolism is the tightly regulated enzyme acetyl-CoA carboxylase (ACC), which catalyzes the carboxylation of acetyl-CoA into malonyl-CoA, a critical metabolic intermediate (Muoio and Newgard, 2006; Saggerson, 2008; Tong, 2005; Wakil and Abu-Elheiga, 2009). Human ACCs are multifunctional enzymes encompassing three distinctive domains, i.e., a biotin carboxylase, a biotin carboxyl carrier protein domain and a carboxyltransferase domain, all essential for stringent regulation of lipid metabolism (Bianchi *et al*., 1990; Cronan and Waldrop, 2002; Tong, 2005; Brownsey *et al*., 2006; Tong, 2013). In lipogenic tissue, malonyl-CoA produced by the ACC1 isoform is utilized for fatty acid synthesis. In the heart and skeletal muscle, malonyl-CoA formed by the ACC2 subtype functions as a negative regulator of fatty acid β-oxidation. ACC2, in particular, has been identified as a potential target for treatment of metabolic syndromes because knockout of ACC2 reduces fat content and increases the resistance to high fat/high carbohydrate–induced obesity and diabetes (Abu-Elheiga *et al*., 1997; Abu-Elheiga *et al*., 2001; Abu-Elheiga *et al*., 2003). Moreover, cardiac-specific deletion of ACC2 prevents metabolic remodeling, underscoring the importance of ACC2 regulation in lipid metabolism (Kolwicz *et al*., 2012). Accordingly, there is increased interest in identifying molecular regulators of ACC-dependent lipid metabolism.

* *Correspondence to: A. Terzic, Mayo Clinic, 200 First Street SW, Rochester, MN 55905, USA.*
E-mail: terzic.andre@mayo.edu

† *This article is published in Journal of Molecular Recognition as part of the virtual Special Issue 'AFM BioMed Shanghai 2013, edited by Jun Hu, SINAP, China and Pierre Parot and Jean-Luc Pellequer, CEA, France'.*

a *S. Park, I.-W. Hwang, E. Perales-Clemente, N. J. Niederländer, A. Terzic*
Center for Regenerative Medicine, Mayo Clinic, Rochester, MN, USA

b *S. Park, I.-W. Hwang, E. Perales-Clemente, N. J. Niederländer, A. Terzic*
Marriott Heart Disease Research Program, Division of Cardiovascular Diseases, Departments of Medicine, Molecular Pharmacology and Experimental Therapeutics, and Medical Genetics, Mayo Clinic, Rochester, MN, USA

c *I.-W. Hwang, Y. Makishima, T. Kato, E. Y. Park*
Laboratory of Biotechnology, Graduate School of Science and Technology, Shizuoka University, Shizuoka, Japan

Spot14 encoded by *Thrsp* has been recognized as a putative regulator of *de novo* lipogenesis (Seelig *et al.*, 1981; Kinlaw *et al.*, 1995). Widely expressed in lipogenic tissues including liver, mammary gland and adipose tissue, *Thrsp* rises rapidly under physiological stimuli and thyroid hormone challenges and is tightly regulated by transcriptional factors, including the sterol regulatory element binding protein and the carbohydrate responsive element binding protein, which activate genes involved in fatty acid synthesis (Mater *et al.*, 1999; Ma *et al.*, 2005; LaFave *et al.*, 2006). Blocking translation of *Thrsp* reduces the levels of lipogenesis associated with the reduction of lipogenic enzymes, including ATP-citrase lyase, fatty acid synthase, malic enzyme and pyruvate kinase (Kinlaw *et al.*, 1995; Brown *et al.*, 1997). Spot14 knockout, with a deletion of the entire coding sequence, has produced early embryonic lethality, yet less disruptive Spot14 knockout has delivered viable offspring with increased and decreased lipogenesis in liver and lactating mammary glands, respectively (Kinlaw *et al.*, 1995; Kinlaw *et al.*, 2006; Aipoalani *et al.*, 2010). Furthermore, Spot14 knockdown by RNA interference in hepatocytes reduces fatty acid synthesis (Aipoalani *et al.*, 2010), suggesting a multifaceted role of Spot14 with unknown molecular targets.

Recently, the direct involvement of Spot14 in fatty acid synthesis has been demonstrated (Colbert *et al.*, 2010; Kim *et al.*, 2010). Spot14 alone is unable to bind to and modulate the activity of ACC1, but Mig12, a Spot14 paralog, binds to ACC, inducing polymerization and promoting the catalytic activity of ACC. Co-expression of Spot14 and Mig12, however, leads to assembly of Spot14/Mig12, which attenuates ACC1 polymerization and enzymatic activity, contributing to the regulation of *de novo* lipogenesis. Although Spot14/Mig12-assisted ACC1 modulation of lipogenesis has been documented, it is unknown whether Spot14/Mig12 affects ACC2, which is mainly expressed in oxidative tissues. Furthermore, the putative molecular mechanism in Spot14/Mig12-dependent ACC2 regulation has not yet been probed.

To address the potential regulatory mechanism defining protein–protein interactions between Spot14/Mig12 and ACC2, we applied here a panel of proteomic methods, including atomic force microscopy (AFM) imaging. We report that the Spot14/Mig12 heterocomplex, not the oligo-heterocomplex, attenuates ACC2 polymerization and demonstrates a sequestering function, providing evidence for a previously unrecognized molecular regulator in lipid metabolism.

MATERIALS AND METHODS

Expression and purification of recombinant Spot14/Mig12 in *Escherichia coli*

The complementary DNA (cDNA) fragments of human Spot14 (146 amino acids) and Mig12 (183 amino acids) were incorporated into a pETDuet-1 bicistronic expression vector (Novagen), containing an N-terminal $(His)_6$-tag on Mig12 and no tag on Spot14. The identity of fusion constructs was confirmed by DNA sequencing (Reyes *et al.*, 2009). The constructs were transformed in *E. coli* BL21(DE3) cells and Spot14/Mig12 proteins purified. Recombinant proteins were enriched from a nickel nitrilotriacetic acid (Ni-NTA) agarose column and then from a HiLoad Superdex 200 size exclusion column using an AKTA FPLC (GE Healthcare) system (Park *et al.*, 2008; Park and Terzic, 2010). Spot14/Mig12 was concentrated using a Centricon (EMD Millipore) concentrator, and the protein concentration was quantified using an extinction coefficient of 42 400 $(Mcm)^{-1}$ at 280 nm. The purity of Spot14/Mig12 was determined by densitometry.

Size-exclusion chromatography with multiangle light scattering, quasi-elastic light scattering and refractive index (SEC/MALS/QELS/RI) detectors

Multidetector SEC/MALS/QELS/RI was performed with an Agilent LC1200 for size exclusion chromatography connected with a Wyatt DAWN HELEOS II multiangle static light scattering detector, a Wyatt QELS dynamic light scattering detector, and a Wyatt Optilab rEX differential refractive index detector (Keck Biophysics Facility, Northwestern University) (Sahin and Roberts, 2012; Striegel and Brewer, 2012). The Superdex 200 10/300 GL size-exclusion column (GE Healthcare) was equilibrated for 18 h with column buffer [50 mM phosphate and 300 mM NaCl (pH 7.5)] at a flow rate of 0.5 ml/min. To confirm the functional integrity of the column and the detectors, a bovine serum albumin standard was prepared at 4 mg/ml in column buffer and centrifuged at 10 000 rpm for 10 min, and then 50 μl of the solution was injected onto the column. The Spot14/Mig12 sample was filtered using a 0.1-μm polyvinylidene difluoride (PVDF) membrane centrifugal filter unit (EMD Millipore), and 50 μl of the filtrate was immediately injected onto the column. Data acquisition and analysis were performed using the ASTRA software package (Wyatt Technologies).

Expression and purification of recombinant ACC2 in silkworm *Bombyx mori*

Heterologous human ACC2 was bioengineered using a *B. mori* nucleopolyhedrovirus (BmNPV) bacmid, an *E. coli* and *B. mori* hybrid shuttle vector, in silkworms. The cDNA fragment of ACC2, excluding the first N-terminal 27 hydrophobic amino acids for membrane attachment sequence and the following stretch of amino acids from 28 to 148 responsible for mitochondrial targeting sequence, was cloned along with a C-terminal Flag tag into a pFastbac1 (Invitrogen) expression vector. Constructs confirmed by DNA sequencing were transformed into *E. coli B. mori* DH10Bac-CP competent cells containing the cysteine protease-deficient BmNPV bacmid (Hiyoshi *et al.*, 2007; Motohashi *et al.*, 2005), following a standard protocol of the Bac-to-Bac Baculovirus Expression System (Invitrogen) (Figure 1) (Luckow *et al.*, 1993). Kanamycin-, tetracycline- and gentamicin-resistant white colonies on LB-agar plates were selected, and then the recombinant BmNPV bacmid containing human ACC2 was purified using the QIAGEN Large-Construct Kit. Identity of recombinant bacmids was confirmed by polymerase chain reaction using M13 forward and reverse sequencing primers and bacmid DNA sequencing. Recombinant BmNPV bacmid was injected into silkworm larvae using a DMRIE-C (Invitrogen) transfection reagent, using a 26-gauge needle. At 7 days post-injection, silkworm fat body was collected and diluted with 1 ml cold Tris-NaCl buffer [50 mM Tris-HCl and 150 mM NaCl (pH 7.5)] containing 0.02% Triton X-100 per fat body. After brief sonication on ice, the crude fat body extracts were centrifuged at 6000 g for 20 min, 4 °C, to remove cellular debris following an additional centrifugation at 30 000 *g* for 30 min, 4 °C. The supernatant was then passed through an anti-Flag M2 affinity agarose gel column (Sigma-Aldrich), washed, and eluted with Tris-NaCl buffer, containing 0 and 100 μg/ml Flag peptide, respectively. Eluted fractions containing ACC2 were pooled

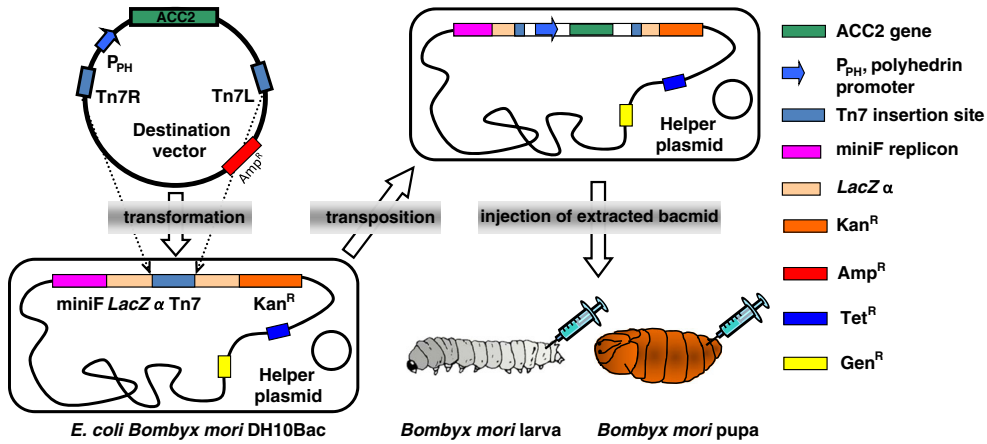

Figure 1. Silkworm-based protein expression platform. The cDNA of human ACC2 was inserted into a destination vector using molecular cloning and then incorporated into the *E. coli B. mori* nucleopolyhedrovirus (BmNPV) bacmid by site-specific transposition of the Tn7 transposon. Recombinant BmNPV bacmid DNA was extracted from *E. coli* for injection into silkworm larvae or pupae for recombinant ACC2 expression.

and stored at −80 °C. Protein concentration was quantified by the Bradford protein assay (Bio-Rad). The purity and integrity of recombinant ACC2 were evaluated by sodium dodecyl sulfate polyacrylamide gel electrophoresis (SDS-PAGE), and Western blot analysis was performed using a monoclonal anti-Flag antibody (Sigma-Aldrich).

Atomic force microscopy

Tapping mode AFM imaging was performed using a Nanoscope IV PicoForce Multimode AFM equipped with an E-scanner and a rectangular-shaped silicon cantilever with a 42 N/m spring constant (Bruker) and a resonant frequency of ~300 kHz at ambient environment (Park *et al*., 2008; Park and Terzic, 2010). Recombinant human ACC2 (10–25 μg/ml) was incubated with or without 10 mM citrate for 20 min at 37 °C. Separately, ACC2 (10–25 μg/ml) was co-incubated with 10 mM citrate and Spot14/Mig12 (5 μg/ml) for 20 min at 37 °C. This incubation mixture was deposited on the freshly cleaved mica surface, incubated for 2 h in a moisture chamber, washed three times with phosphate-buffered saline (PBS) and three times with water, and gently dried under nitrogen stream. Images (512 × 512 pixels/image) were obtained from each sample with maximum image size of 2 × 2 μm. All displayed images represent flattened raw data. Height images were used for measurements of lateral dimensions of proteins, and analysis was performed using the Nanoscope Analysis version 1.40 software (Bruker). For particle analysis, particles were visually inspected to set the threshold height in order to quantitate diameter, area, total number of particles, and a display correlation histogram of particles above the set point value. The absolute in *x*-axis setting was selected in depth histograms.

Acetyl-CoA carboxylase assays

Human ACCs are multifunctional enzymes harboring three distinctive domains, i.e., a biotin carboxylase, a biotin carboxyl carrier protein domain and a carboxyltransferase domain (Bianchi *et al*., 1990; Cronan and Waldrop, 2002; Tong, 2005; Brownsey *et al*., 2006; Tong, 2013). Biotin carboxylase catalyzes the adenosine triphosphate (ATP)–dependent carboxylation of biotin using bicarbonate as the donor of the carboxyl group (Tong, 2005; Chou *et al*., 2009). We measured ACC2 activity based on ATP-dependent biotin carboxylase activity, which catalyzed ATP into adenosine diphosphate (ADP) and inorganic phosphate. Assays were performed in 190 μl of 50 mM HEPES, 10 mM $MgCl_2$, 5 mM $NaHCO_3$, 10 mM sodium citrate, 0.2 mM acetyl-CoA, 1 mM biotin, and 2 mM ATP (pH 7.5). Reactions were initiated by the addition of 10 μl of purified ACC2, continued for 30 min at 37 °C, and then terminated by the addition of 200 μl of 12% SDS. Produced organic phosphate was detected by colorimetry (Park *et al*., 2008; Park and Terzic, 2010). In a separate set of experiments, ACC2 activity was measured in the presence of recombinant Spot14/Mig12.

Blue native-PAGE (BN-PAGE) and Western blotting

Recombinant Flag-tagged ACC2 (2–5 μg) was incubated at 37 °C for 10 min with 1 μg of Spot14/Mig12 in the presence and absence of 1 mM citrate in Tris-NaCl buffer with 5 mM dithiothreitol. In separate experiments, recombinant ACC2 was incubated with 1 mM citrate at 37 °C for 5 min, followed by an additional 10 min of incubation with an addition of Spot14/Mig12. After incubation, 3 μl of loading buffer containing 5% Coomassie G-250, 1 M 6-aminohexanoic acid, and 10 mM Bis-Tris pH 7 was added to each 12 μl of reaction mixture, which was subjected to non-denaturing BN-PAGE using a 3%–12% gradient NativePAGE Novex Bis-Tris Gel (Invitrogen). Native gel uses Coomassie G-250 as a charge-shift molecule (Wittig *et al*., 2006). Resolved proteins were transferred by electrophoresis onto 0.2-μM Immun-Blot PVDF membranes (Bio-Rad), and excess Coomassie G-250 was removed from the membranes by sequential washing with methanol and TBS-T (Tris-NaCl buffer with 0.1% Tween 20). The membranes were incubated with 5% non-fat dried milk in TBS-T, and using a monoclonal anti-Flag antibody (Sigma-Aldrich), immunoblot analysis was performed. Antibody-bound proteins were counterstained using horseradish peroxidase–conjugated secondary antibody and then detected using SuperSignal West Pico or West Femto (Pierce) (Karger *et al*., 2008; Olson *et al*., 2006).

Production of lenti-Spot14 and lenti-Mig12 viruses

The human cDNA of Mig12 and Spot14 were cloned into a multiple attenuated human immunodeficiency virus (HIV)-based lentiviral vector for HEK293T cell transfection to produce virus particles. In order to ensure biosafety when handling HIV-based lentiviruses and to prevent viral replication *in vivo*, a three-component plasmid method was utilized composed of a bicistronic plasmid carrying

the gene of interest and enhanced green fluorescent protein (eGFP) as a marker (pHR-SIN-BX-IRES-Em), a helper plasmid expressing the vesicular stomatitis virus glycoprotein (VSV-G) (pMD-G) and a packaging plasmid (pCMVR8.91) expressing GAG and POL (Ikeda *et al*., 2003; Ahmed *et al*., 2008; Sakuma *et al*., 2012). HEK293T cells were transfected with plasmids to generate replication-deficient and self-inactivating lentiviral particles using the FuGENE 6 transfection reagent (Roche) following standard protocols (Naldini *et al*., 1996; Zufferey *et al*., 1997; Ikeda *et al*., 2003). Strep-tagged Spot14 or Flag-tagged Mig12 and eGFP proteins were co-expressed in the same cells using the bicistronic pHR-SIN-BX-IRES-Spot14 (or -Mig12) expression vector. As a control, bicistronic vector (pHR-SIN-BX-IRES-Em) expressing eGFP alone was used. On day 3 or 4 after transfection, VSV-G–pseudotyped high-titer lentiviruses were collected from culture supernatants and concentrated about 1000-fold by ultracentrifugation. Viral titer was determined by counting the number of GFP-positive HEK293T cells infected through a series of dilution of the concentrated lentiviruses.

Stable expression of Spot14 and Mig12 proteins using lentiviruses

HEK293T cells were infected with high-titer lentiviruses (multiplicity of infection (MOI) of 5) that produced Spot14, Mig12 or Spot14/Mig12 in the presence of 5 μg/ml of polybrene. After overnight culture with lentivirus, cells were washed and incubated in fresh culture medium. At 3 days post-infection, transduction efficiency was evaluated using GFP. To check for stable expression of Spot14 and Mig12 from the transduced cells, Western blot analysis was performed. Cultured cells were washed two times with PBS, incubated with cell lysis buffer (Cell Signaling) for 5 min on ice, and then scraped to collect cells. After sonication, crude extracts were centrifuged at 14 000 g in a cold table top centrifuge, and the resulting supernatant was collected and stored at −80 °C. ACC2 expression and polymerization, and Spot14 or Mig12 incorporation into ACC were probed using immunoblot analyses using a monoclonal antibody of acetyl-CoA carboxylase 2 (Cell Signaling), anti-Flag (Sigma-Aldrich), Strep●Tag (EMD Millipore) and Spot14 (Santa Cruz Biotech). Typically, 10 μg of the total protein from HEK293T cell extracts was used for gradient BN-PAGE.

RESULTS

Structural integrity of Spot14/Mig12

Using a bicistronic vector, Spot14/Mig12 was co-expressed in *E. coli*, and purified with a Ni-NTA column and then with a Superdex 200 size-exclusion column chromatography. Based on molecular weight standards in gel filtration chromatography, recombinant Spot14/Mig12 was produced as a heterocomplex (αβ) and an oligo-heterocomplex $(\alpha\beta)_n$, displaying >93% purity and migrated at the corresponding molecular weight on SDS-PAGE (Figure 2A). No equilibrium shift was detected between the heterocomplex and the oligo-heterocomplex analyzed in size-exclusion chromatography.

Multidetector SEC/MALS/QELS/RI was utilized to evaluate the molecular composition of recombinant Spot14/Mig12 eluted from a Superdex 200 column. SEC/MALS/QELS/RI determines

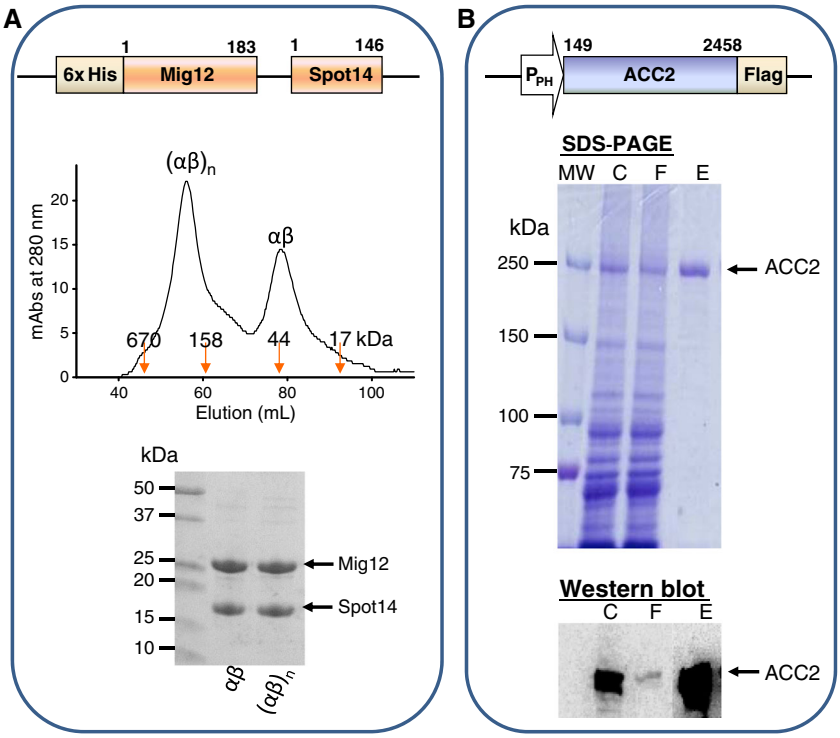

Figure 2. Structural integrity of ACC2 and Spot14/Mig12. (A) Human Spot14/Mig12 was expressed in *E. coli* with an amino-terminal 6x histidine tag and purified by Ni-affinity and size exclusion chromatography, producing oligo-heterocomplex and heterocomplex proteins verified by molecular weight standards. Mig12 (21.8 kDa) and Spot14 (16.5 kDa) migrated at their expected molecular weights on SDS-PAGE. (B) Human ACC2 was expressed in silkworm *B. mori* fat body with a carboxyl-terminal Flag tag and purified from an anti-Flag M2 affinity agarose gel column. SDS-PAGE of Coomassie blue-stained ACC2 (261 kDa) migrated at a corresponding molecular weight. The identity of ACC2 was confirmed by immunoblot analysis using a monoclonal anti-Flag antibody. C, crude extract of silkworm fat body; F, flow through from an anti-Flag affinity column; E, elution fractions.

the absolute molar mass and average size of particles in solution by measuring the characteristics of scattered light from the sample (Sahin and Roberts, 2012; Striegel and Brewer, 2012). The heterocomplex resolved monodisperse and homogeneous particles whereas the oligo-heterocomplex separated into four different components (Figure S1 in the Supplementary Material). The observed molar mass at the apex of the heterocomplex peak was 39.01 kDa, which is less than 2% off from the theoretical molecular mass of the Spot14/Mig12 heterocomplex, confirming the molecular composition. In contrast, the oligo-heterocomplex resolved into dodeca-, hexa-, tetra-, and di-heterocomplexes, where the predominant species was a hexa-heterocomplex. Based on these analyses, we designated Spot14/Mig12 components into heterocomplex ($\alpha\beta$) and hexa-heterocomplex $(\alpha\beta)_6$.

Human acetyl-CoA carboxylase production in silkworm

Human acetyl-CoA carboxylase 2 (ACC2), an ACC isoform abundantly present in the heart and skeletal muscle, was expressed in silkworm *B. mori* with a Flag purification tag (Figure 2B). Binding to an anti-Flag M2 affinity agarose gel column (Sigma-Aldrich) was targeted by a Flag tag, with Flag peptide elution yielding enriched purity of ACC2 (>93%) compared to fat body extracts and washed fractions. Detected at corresponding molecular weight on SDS-PAGE, the expressed ACC2 was validated with immunoblotting using an anti-Flag antibody. In addition, silkworm-based protein expression provided a high yield of purified ACC2 (0.15 mg/silkworm) with a specific activity of 21.4 ± 1.4 nmol/mg/min ($n = 5$), similar to reported values (Kim *et al*., 2007). Thus, human ACC2 expressed in silkworm harbors consistent enzymatic activity, underscoring that the silkworm-based protein expression system provides a reliable platform for eukaryotic ACC2 production.

ACC2 and Spot14/Mig12 interactions

Acetyl-CoA carboxylase is modulated by multiple regulatory factors (Thampy and Wakil, 1988; Wakil and Abu-Elheiga, 2009). Phosphorylation of ACC by adenosine monophosphate (AMP)–-activated protein kinase inactivates enzymatic activity whereas dephosphorylation activates the enzyme promoting polymerization. ACC is also allosterically activated by a high concentration of citrate, which induces the polymerization of an inactive protomeric form into an active filamentous form with increased functional activity (Beaty and Lane, 1983; Gregolin *et al*., 1966; Kim *et al*., 2007). Without citrate, recombinant ACC bioengineered in a baculovirus/Sf9 cell expression system or ACC isolated from tissue does not show any detectable catalytic activity (Thampy and Wakil, 1988; Cheng *et al*., 2007).

The structural properties of human ACC2 modulated by citrate were evaluated by mapping the architecture of purified proteins derived from silkworm *B. mori* using AFM at a nanoscale resolution (Figure 3). ACC2 alone demonstrated almost homogeneous island-like topographies, whereas when citrate was added to

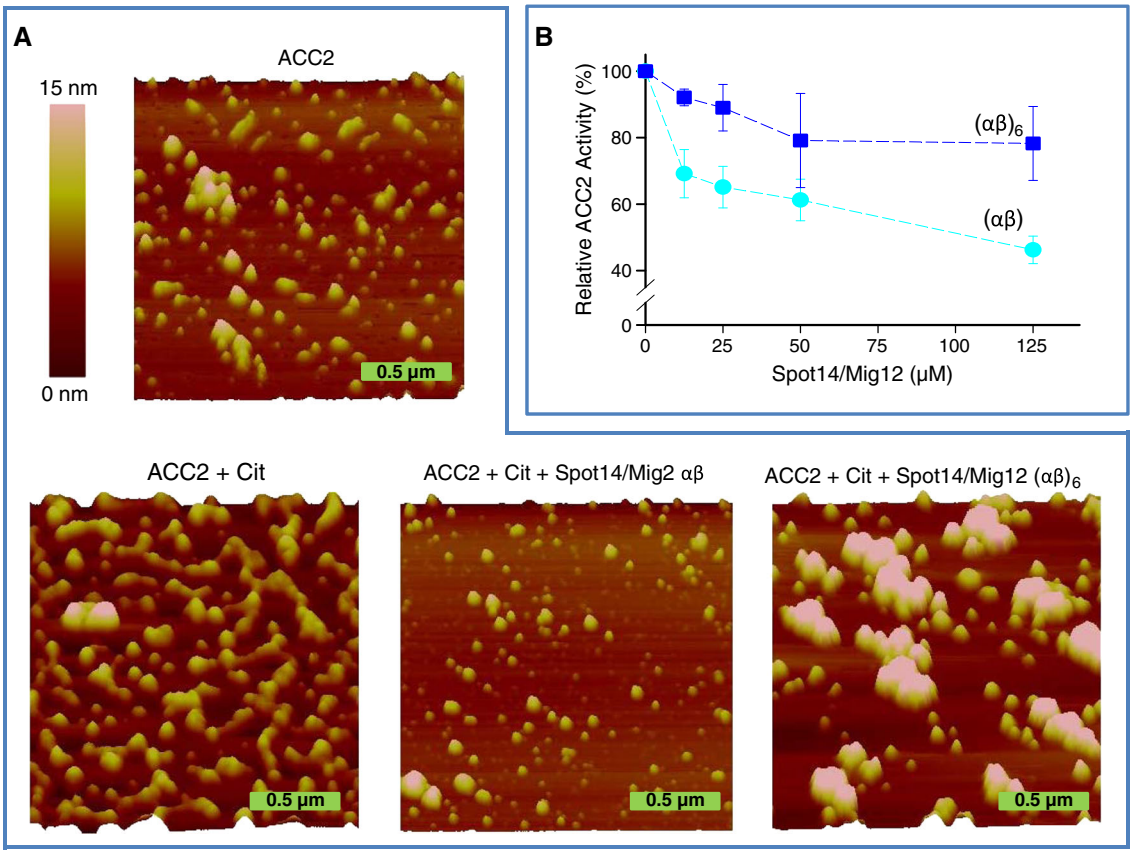

Figure 3. Structural and functional modulation of ACC2. (A) AFM nanoscale imaging was obtained for ACC2 alone, ACC2 + citrate, ACC2 + citrate + Spot14/Mig12 $\alpha\beta$, and ACC2 + citrate + Spot14/Mig12 $(\alpha\beta)_6$ after 20 min incubation at 37 °C. Citrate induced ACC2 polymerization producing microfilaments. Spot14/Mig12 $\alpha\beta$ and $(\alpha\beta)_6$ suppressed complete and partial ACC2 polymerization, respectively. Height image of the AFM data is shown with a 15-nm color height scale. (B) Activity of recombinant ACC2 was measured in the presence of different Spot14/Mig12 concentrations. Cit, citrate.

ACC2, filamentous polymers of ACC2 were produced. To quantitate structural changes of ACC2 induced by citrate, two distinctive structural properties, diameter and area, were evaluated using the Nanoscope particle analysis software (Figure 4 and Figure S2 in the Supplementary Material). ACC2 alone demonstrated particle distribution that was 58 ± 4 nm in diameter and 3395 ± 365 nm^2 ($n = 152$) in area, whereas citrate-induced ACC2 produced filamentous polymeric particles that were 129 ± 9 nm in diameter and 19 659 ± 4851 nm^2 ($n = 70$) in area, revealing significant topographic changes of ACC2 produced by citrate (Figures 3 and 4; Table 1). Thus, high-resolution AFM imaging and citrate-induced ACC2 polymerization validated the functional integrity of recombinant ACC2 generated with high fidelity in silkworm *B. mori*.

To resolve the putative protein–protein interactions between Spot14/Mig12 and ACC2, AFM imaging and functional assays were employed (Figures 3 and 4). As Spot14/Mig12 was expressed as heterocomplexes and hexa-heterocomplexes, these proteins were incubated with citrate and ACC2. The ensuing microarchitecture revealed completely and partially dispersed polymeric ACC2 nanostructures, much larger than the Spot14/Mig12 hexa-heterocomplex alone (Figure S3 in the Supplementary Material and Table 1). When a Spot14/Mig12 heterocomplex was free to interact with ACC2 in the presence of citrate, the inhibition of citrate-induced ACC2 polymerization stood out, conspicuously producing particles that were 49 ± 3 nm in diameter and 2269 ± 150 nm^2 ($n = 165$) in area (Table 1). These topographic values are significantly smaller than those of citrate-induced ACC2 and almost identical to ACC2 alone. In contrast, when a Spot14/Mig12 hexa-heterocomplex was incubated with ACC2 in the presence of citrate, citrate-induced ACC2 polymerization was partially inhibited accompanying the production of supra-macromolecular complexes (Figures 3 and 4; Table 1). Consistent with topographic mapping indicative of reduced polymerization, the ACC2 enzymatic activity was significantly restrained with the addition of the Spot14/Mig12 heterocomplex compared to a modest modulation by the hexa-heterocomplex counterpart (Figure 3B). Thus, the Spot14/Mig12 heterocomplex is a designated molecular unit responsible for the suppression of human ACC2 polymerization and function.

Capping function of Spot14/Mig12 in ACC2 polymerization

Regulation of ACC2 polymerization by the Spot14/Mig12 heterocomplex was further evaluated using gradient BN-PAGE (Figure 5). As Spot14/Mig12 inhibits ACC2 polymerization, the addition of Spot14/Mig12 to ACC2 would immobilize the polymerization process regardless of the ACC2 polymerization steps. Incubation of recombinant ACC2 with citrate induced the formation of high-molecular-weight ACC2 polymers, but incubation of ACC2 with citrate and the Spot14/Mig12 heterocomplex reduced ACC2 polymer formation, supporting AFM studies (Figure 5A). However, Spot14/Mig12 addition to the nucleated ACC2 polymers induced by citrate during pre-incubation could neither arrest the polymerization process nor depolymerize polymeric ACC2 back to lower molecular weight components (Figure 5B). These findings demonstrate a capping function of the Spot14/Mig12 heterocomplex, preventing ACC2 nucleation during filamentous polymer formation.

The sequestering function of Spot14/Mig12 in ACC2 polymerization was further validated in cell culture using a lentiviral protein expression system. Strep-tagged Spot14 and Flag-tagged Mig12 were produced individually or co-produced in the HEK293T cells using bicistronic pHR-SIN-BX-IRES-Spot14 (or -Mig12) expression lentivirus vector. Bicistronic vector (pHR-SIN-BX-IRES-Em) expressing eGFP alone was used as a control expression

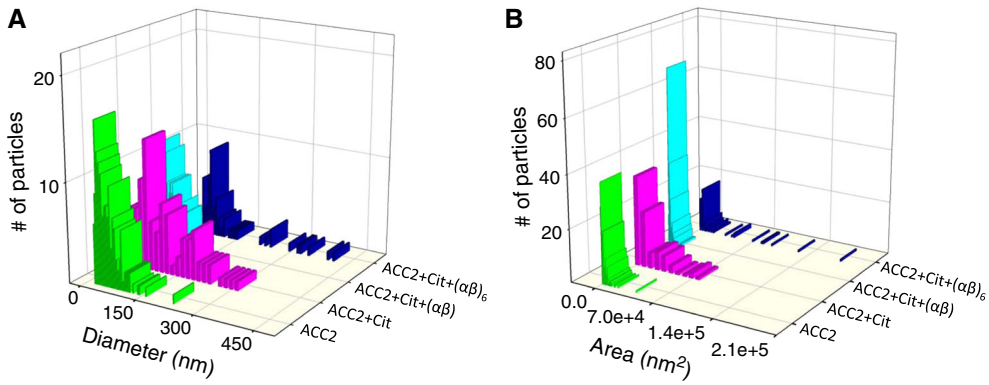

Figure 4. Diameter (A) and area (B) analyses of AFM height images produced by ACC2 alone, ACC2 + citrate, ACC2 + citrate + Spot14/Mig12 αβ, and ACC2 + citrate + Spot14/Mig12 $(\alpha\beta)_6$. Cit, citrate; αβ, Spot14/Mig12 heterocomplex; $(\alpha\beta)_6$, Spot14/Mig12 hexa-heterocomplex.

Table 1. Particle analysis by AFM

	Diameter (nm)	Area (nm^2)	
Human ACC2	58 ± 4	3395 ± 365	($n = 152$)
Human ACC2 + citrate	129 ± 9	19 659 ± 4,851	($n = 70$)
Human ACC2 + citrate + Spot14/Mig12, αβ	49 ± 3	2269 ± 150	($n = 165$)
Human ACC2 + citrate + Spot14/Mig12, $(\alpha\beta)_6$	127 ± 13	19 981 ± 4,564	($n = 50$)
Spot14/Mig12, $(\alpha\beta)_6$	28 ± 2	822 ± 125	($n = 51$)

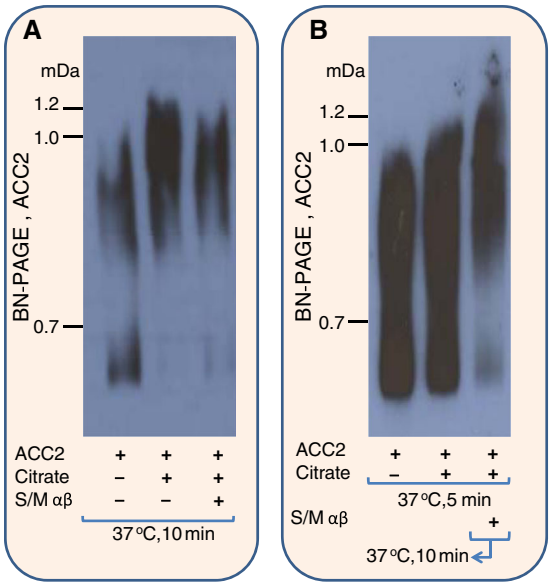

Figure 5. Spot14/Mig12 heterocomplex prevents ACC2 polymerization. ACC2 polymerization with citrate or citrate + Spot14/Mig12 αβ was initially separated by gradient BN-PAGE and analyzed by Western blot using an anti-Flag antibody. (A) Incubation of ACC2 with citrate induced formation of high-molecular-weight ACC2 polymers, but addition of Spot14/Mig12 αβ diminished the generation of ACC2 polymers. (B) ACC2 and citrate were pre-incubated to produce nucleated ACC2 polymers, followed by additional incubation with Spot14/Mig12 αβ. Spot14/Mig12 heterocomplex addition could not further halt the polymerization process of nucleated ACC2 polymers. S/M αβ, Spot14/Mig12 heterocomplex.

system. Bright field and fluorescence microscopy displayed confluent cell growth and eGFP protein production from lentivirus transfection, in addition to wild type cells without transfection (Figure 6A). Moreover, expression of Spot14 and Mig12 in HEK293T cells was confirmed by Western blot analysis using Spot14 and anti-Flag M2 antibodies, respectively (Figure 6B). The effects of ACC2 expression and polymerization by Spot14 and Mig12 were examined using the immunoblotting of gradient BN-PAGE. High-molecular-weight ACC2 polymers were produced in all samples, including control, but the abundance of ACC2 expression was reduced when Spot14 was transfected or co-transfected with Mig12 (Figure 6C). In addition, Mig12 transfection produced significant Mig12 incorporation into ACC, yet co-transfection of Spot14 and Mig12 reduced Mig12 integration into ACC. In particular, when Spot14 incorporation into ACC was probed using Spot14 specific anti-Strep II and Spot14 antibodies, no band was detected, underscoring that polymerized ACC does not incorporate Spot14/Mig12. Taken together, these data indicate that the Spot14/Mig12 heterocomplex functions as a capping molecule of ACC2, preventing an initial polymerization process.

DISCUSSION

Lipid metabolism is an integral metabolic process to maintain dynamic cellular functions (Wakil and Abu-Elheiga, 2009; Lopaschuk *et al*., 2010; Folmes *et al*., 2013; Knobloch *et al*., 2013). Acetyl-CoA carboxylase regulates a first and rate-limiting step in lipid metabolism by catalyzing the carboxylation of acetyl-CoA to produce malonyl-CoA, a crucial metabolite in modulating anabolic lipogenesis and catabolic fatty acid β-oxidation (Muoio and Newgard, 2006; Saggerson, 2008; Wakil and Abu-Elheiga, 2009). Two different isoforms of acetyl-CoA carboxylase, ACC1 and ACC2, partake in fatty acid metabolism—ACC1 for lipogenesis and ACC2 for fatty acid oxidation (Abu-Elheiga *et al*., 1995; Saggerson, 2008; Wakil and Abu-Elheiga, 2009). In particular, the regulation of ACC2 has been associated with metabolic dysfunctions and metabolic remodeling (Abu-Elheiga *et al*., 2001; Abu-Elheiga *et al*., 2003; Abu-Elheiga *et al*., 2012; Kolwicz *et al*., 2012). Here, high-resolution AFM imaging and biochemical analysis were employed to resolve the molecular mechanism underlying protein–protein interactions between Spot14/Mig12 and ACC2. The Spot14/Mig12 heterocomplex-induced suppression of ACC2 polymerization and function unveils a molecular regulator of ACC2 and associated lipid metabolism.

Malonyl-CoA is recognized as a molecular rheostat adjusting *de novo* lipogenesis and oxidative mitochondrial energy metabolism (Tong, 2005; Saggerson, 2008; Wakil and Abu-Elheiga, 2009; Reyes *et al*., 2010; Wolfgang and Lane, 2011; Folmes *et al*., 2013). In non-lipogenic tissue such as the skeletal and heart muscle, where ACC2 is abundantly expressed, malonyl-CoA allosterically inhibits carnitine palmitoyltransferase (CPT1), an integral membrane protein associated with the mitochondrial outer membrane catalyzing the transfer of long-chain fatty acid into the mitochondria as the rate-limiting step of fatty acid β-oxidation. Thus, operating as a suppressing molecule of ACC2 polymerization and function, although speculative, Spot14/Mig12 might regulate energy metabolism in oxidative tissues.

Atomic force microscopy imaging at a nanoscale resolution and functional catalytic assays provided an approach to reveal the molecular functional unit of Spot14/Mig12 responsible for ACC2 regulation. Incubation of ACC2, citrate and the Spot14/Mig12 heterocomplex produced an inclusive suppression of citrate-induced ACC2 polymerization in contrast with the less efficient Spot14/Mig12 hexa-heterocomplex incubation (Figure 7). However, the nucleated ACC2 polymers assembled during pre-incubation produced microfilaments despite Spot14/Mig12 addition. Moreover, Spot14 incorporation into polymerized ACC was not detected in cultured cells, demonstrating that the Spot14/Mig12 heterocomplex is a designated capping molecule of ACC2 thereby preventing further polymerization.

Crystallographic symmetry of Spot14 crystals suggests an assembly of higher-order oligomers (Krissinel and Henrick, 2007; Colbert *et al*., 2010). In light of this, a recombinant Spot14/Mig12 hexa-heterocomplex was produced, which was less effective in modulating ACC2 function and polymerization. Although the distinctive function of Spot14 oligomer has not been identified, Spot14 oligomer might be involved in the regulation of fatty acid movement or function as a trafficking protein, physically linking different steps of lipogenesis (LaFave *et al*., 2006). Thus, the main function of Spot14/Mig12 oligomers could be in the modulation of upstream lipogenesis mechanisms, in addition to partial ACC2 regulation.

Acetyl-CoA carboxylase is regulated by multiple factors, including covalent modification by phosphorylation/dephosphorylation, whereby phosphorylation inactivates ACC activity whereas dephosphorylation activates the enzyme (Shen *et al*., 2004; Wakil and Abu-Elheiga, 2009). Based on the crystal structure of the biotin carboxylase domain of ACC2, phosphorylation-regulated polymerization has been proposed (Cho *et al*., 2010). Phosphorylated Ser222 binds to the putative dimer interface of the biotin carboxylase domain, disrupting polymerization by inhibiting the interactions between the ACC2 dimer interfaces of the neighboring

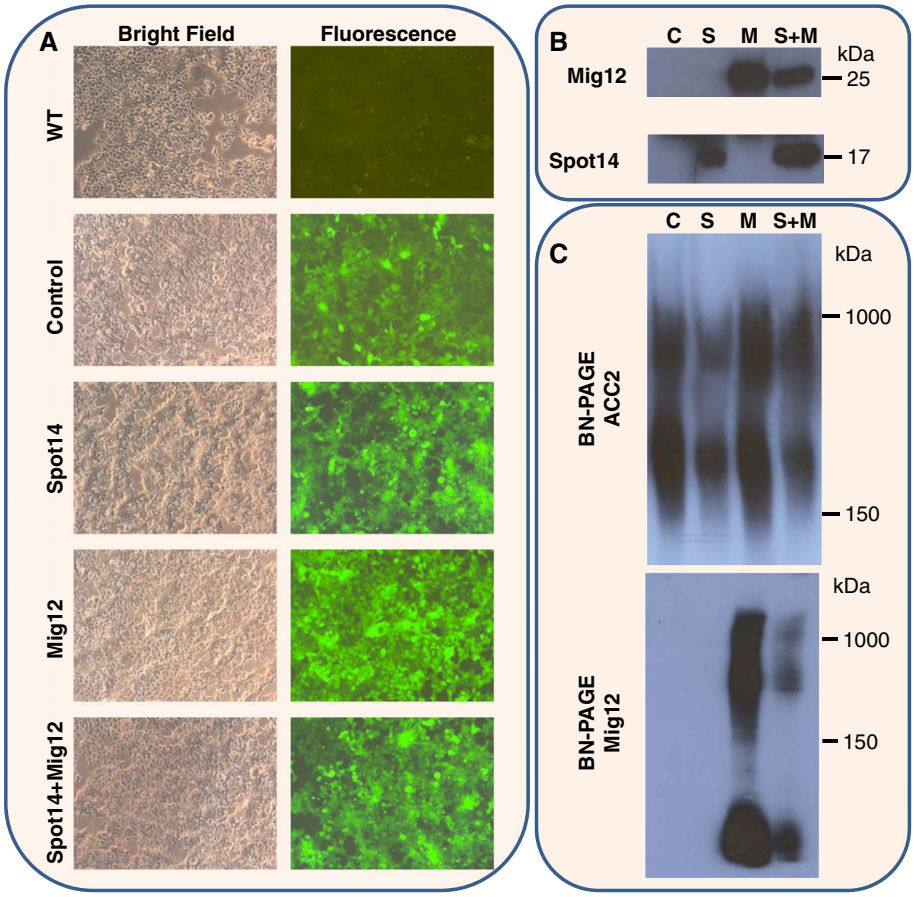

Figure 6. Spot14/Mig12 sequesters ACC2 polymerization in cultured cells. (A) Cultured HEK293T cells were imaged by bright and fluorescence microscopy, alone or following transfection with control or bicistronic pHR-SIN-BX-IRES-Spot14 (or -Mig12) lentiviruses, co-expressing eGFP. (B) HEK293T cell lysates were resolved by SDS-PAGE and analyzed by Western blot using a monoclonal antibody of anti-Flag (Mig12) and Spot14. (C) HEK293T cell lysates were resolved by gradient BN-PAGE and analyzed by Western blot using a monoclonal antibody of ACC2 and anti-Flag (Mig12). Transfection of Spot14 or co-transfection of Spot14 and Mig12 decreased ACC2 expression. In addition, integration of Mig12 into ACC2 polymers was significantly suppressed when Spot14 and Mig12 was co-transfected. C, control transfection; S, Spot14 transfection; M, Mig12 transfection; S + M, Spot14 + Mig12 co-transfection.

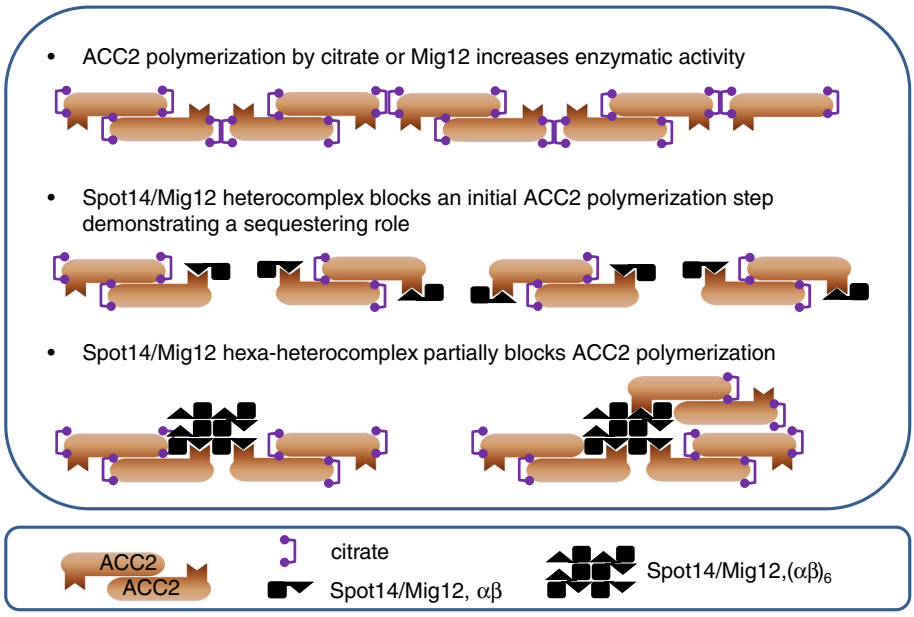

Figure 7. A schematic summary of ACC regulation by Spot14/Mig12. Polymerization of ACC by citrate or Mig12 increases catalytic activity. ACC polymerization and its catalytic function are inhibited by the Spot14/Mig12 heterocomplex, more effective than the oligo-heterocomplex.

biotin carboxylase domains. Thus, it is worth noting that a Spot14/Mig12 heterocomplex might bind to a biotin carboxylase domain, resulting in conformational and structural hindrance for polymerization.

Silkworm *B. mori*, recognized as a natural bioreactor to produce silk, is an emerging host for recombinant protein production (Maeda *et al*., 1985; Tamura *et al*., 2000; Tomita *et al*., 2003 Kato *et al*., 2010; Teule *et al*., 2012;). Silkworm provides a post-translational modification machinery including glycosylation, phosphorylation and disulfide bond formation, all essential for soluble and correctly folded recombinant eukaryotic proteins (Park *et al*., 2007; Dojima *et al*., 2009; Kato *et al*., 2010; Vandenborre *et al*., 2011). Using a BmNPV bacmid, an *E. coli* and *B. mori* hybrid shuttle vector, authentic recombinant proteins are readily expressed by direct injection of recombinant bacmid into silkworm pupae and larvae, reducing the time required for pre-production virus amplification in cultured cells. Moreover, protein expression levels in silkworm are consistently high (Dojima *et al*., 2009; Ogata *et al*., 2009; Park *et al*., 2009 Kato *et al*., 2010;). To exploit the advantages of silkworm-based protein expression system, human ACC2, a multifunctional enzyme composed of several distinctive domains, was expressed. Indeed, silkworm-based protein production exhibits a high yield of purified protein (0.15 mg/silkworm), which retains catalytic activity and citrate-induced polymerization, underscoring that silkworm serves as a protein expression host to generate high-fidelity recombinant eukaryotic protein.

In summary, regulation of a multifunctional ACC2 by Spot14/Mig12 was resolved using nanoscale AFM imaging and biochemical assays. Recombinant ACC2 from silkworm displayed authentic polymerization and functional activity, which were inhibited by the Spot14/Mig12 heterocomplex. Moreover, as a molecular substrate for ACC2, the Spot14/Mig12 heterocomplex revealed a sequestering function in preventing the function and initial polymerization of ACC2. Thus, deconvoluted protein–protein interactions shed light on a previously unrecognized molecular regulator potentially useful in modulating catalytic lipid metabolism.

Acknowledgements

Authors express their gratitude to Dr. Leonid Zingman for expert discussions. This work was supported by the National Institutes of Health; Marriott Heart Disease Research Program, Mayo Clinic; and Young Research Overseas Dispatches Program for Accelerating Brain Circulation, Japan Society for the Promotion of Science. A.T. holds the Marriott Family Professorship in Cardiovascular Diseases Research.

REFERENCES

Abu-Elheiga L, Jayakumar A, Baldini A, Chirala SS, Wakil SJ. 1995. Human acetyl-CoA carboxylase: characterization, molecular cloning, and evidence for two isoforms. *Proc. Natl. Acad. Sci. U. S. A.* **92**: 4011–4015.

Abu-Elheiga L, Almarza-Ortega DB, Baldini A, Wakil SJ. 1997. Human acetyl-CoA carboxylase 2. Molecular cloning, characterization, chromosomal mapping, and evidence for two isoforms. *J. Biol. Chem.* **272**: 10669–10677.

Abu-Elheiga L, Matzuk MM, Abo-Hashema KA, Wakil SJ. 2001. Continuous fatty acid oxidation and reduced fat storage in mice lacking acetyl-CoA carboxylase 2. *Science* **291**: 2613–2616.

Abu-Elheiga L, Oh W, Kordari P, Wakil SJ. 2003. Acetyl-CoA carboxylase 2 mutant mice are protected against obesity and diabetes induced by high-fat/high-carbohydrate diets. *Proc. Natl. Acad. Sci. U. S. A.* **100**: 10207–10212.

Abu-Elheiga L, Wu H, Gu Z, Bressler R, Wakil SJ. 2012. Acetyl-CoA carboxylase $2^{-/-}$ mutant mice are protected against fatty liver under high-fat, high-carbohydrate dietary and de novo lipogenic conditions. *J. Biol. Chem.* **287**: 12578–12588.

Ahmed AU, Schmidt RL, Park CH, Reed NR, Hesse SE, Thomas CF, Molina JR, Deschamps C, Yang P, Aubry MC, Tang AH. 2008. Effect of disrupting seven-in-absentia homolog 2 function on lung cancer cell growth. *J. Natl. Cancer Inst.* **100**: 1606–1629.

Aipoalani DL, O'Callaghan BL, Mashek DG, Mariash CN, Towle HC. 2010. Overlapping roles of the glucose-responsive genes, S14 and S14R, in hepatic lipogenesis. *Endocrinology* **151**: 2071–2077.

Beaty NB, Lane MD. 1983. The polymerization of acetyl-CoA carboxylase. *J. Biol. Chem.* **258**: 13051–13055.

Bianchi A, Evans JL, Iverson AJ, Nordlund AC, Watts TD, Witters LA. 1990. Identification of an isozymic form of acetyl-CoA carboxylase. *J. Biol. Chem.* **265**: 1502–1509.

Brown SB, Maloney M, Kinlaw WB. 1997. "Spot 14" protein functions at the pretranslational level in the regulation of hepatic metabolism by thyroid hormone and glucose. *J. Biol. Chem.* **272**: 2163–2166.

Brownsey RW, Boone AN, Elliott JE, Kulpa JE, Lee WM. 2006. Regulation of acetyl-CoA carboxylase. *Biochem. Soc. Trans.* **34**: 223–227.

Cheng D, Chu CH, Chen L, Feder JN, Mintier GA, Wu Y, Cook JW, Harpel MR, Locke GA, An Y, Tamura JK. 2007. Expression, purification, and characterization of human and rat acetyl coenzyme A carboxylase (ACC) isozymes. *Protein Expr. Purif.* **51**: 11–21.

Cho YS, Lee JI, Shin D, Kim HT, Jung HY, Lee TG, Kang LW, Ahn YJ, Cho HS, Heo YS. 2010. Molecular mechanism for the regulation of human ACC2 through phosphorylation by AMPK. *Biochem. Biophys. Res. Commun.* **391**: 187–192.

Chou CY, Yu LP, Tong L. 2009. Crystal structure of biotin carboxylase in complex with substrates and implications for its catalytic mechanism. *J. Biol. Chem.* **284**: 11690–11697.

Colbert CL, Kim CW, Moon YA, Henry L, Palnitkar M, McKean WB, Fitzgerald K, Deisenhofer J, Horton JD, Kwon HJ. 2010. Crystal structure of Spot 14, a modulator of fatty acid synthesis. *Proc. Natl. Acad. Sci. U. S. A.* **107**: 18820–18825.

Cronan JE, Jr., Waldrop GL. 2002. Multi-subunit acetyl-CoA carboxylases. *Prog. Lipid Res.* **41**: 407–435.

Dojima T, Nishina T, Kato T, Uno T, Yagi H, Kato K, Park EY. 2009. Comparison of the *N*-linked glycosylation of human β1,3-*N*-acetylglucosaminyltransferase 2 expressed in insect cells and silkworm larvae. *J. Biotechnol.* **143**: 27–33.

Folmes CD, Park S, Terzic A. 2013. Lipid metabolism greases the stem cell engine. *Cell Metab.* **17**: 153–155.

Gregolin C, Ryder E, Kleinschmidt AK, Warner RC, Lane MD. 1966. Molecular characteristics of liver acetyl CoA carboxylase. *Proc. Natl. Acad. Sci. U. S. A.* **56**: 148–155.

Hiyoshi M, Kageshima A, Kato T, Park EY. 2007. Construction of a cysteine protease deficient *Bombyx mori* multiple nucleopolyhedrovirus bacmid and its application to improve expression of a fusion protein. *J. Virol. Methods* **144**: 91–97.

Ikeda Y, Takeuchi Y, Martin F, Cosset FL, Mitrophanous K, Collins M. 2003. Continuous high-titer HIV-1 vector production. *Nat. Biotechnol.* **21**: 569–572.

Karger AB, Park S, Reyes S, Bienengraeber M, Dyer RB, Terzic A, Alekseev AE. 2008. Role for SUR2A ED domain in allosteric coupling within the K_{ATP} channel complex. *J. Gen. Physiol.* **131**: 185–196.

Kato T, Kajikawa M, Maenaka K, Park EY. 2010. Silkworm expression system as a platform technology in life science. *Appl. Microbiol. Biotechnol.* **85**: 459–470.

Kim KW, Yamane H, Zondlo J, Busby J, Wang M. 2007. Expression, purification, and characterization of human acetyl-CoA carboxylase 2. *Protein Expr. Purif.* **53**: 16–23.

Kim CW, Moon YA, Park SW, Cheng D, Kwon HJ, Horton JD. 2010. Induced polymerization of mammalian acetyl-CoA carboxylase by MIG12 provides a tertiary level of regulation of fatty acid synthesis. *Proc. Natl. Acad. Sci. U. S. A.* **107**: 9626–9631.

Kinlaw WB, Church JL, Harmon J, Mariash CN. 1995. Direct evidence for a role of the "spot 14" protein in the regulation of lipid synthesis. *J. Biol. Chem.* **270**: 16615–16618.

Kinlaw WB, Quinn JL, Wells WA, Roser-Jones C, Moncur JT. 2006. Spot 14: A marker of aggressive breast cancer and a potential therapeutic target. *Endocrinology* **147**: 4048–4055.

Knobloch M, Braun SM, Zurkirchen L, von Schoultz C, Zamboni N, Arauzo-Bravo MJ, Kovacs WJ, Karalay O, Suter U, Machado RA, Roccio M, Lutolf MP, Semenkovich CF, Jessberger S. 2013. Metabolic control of adult neural stem cell activity by Fasn-dependent lipogenesis. *Nature* **493**: 226–230.

Kolwicz SC, Jr., Olson DP, Marney LC, Garcia-Menendez L, Synovec RE, Tian R. 2012. Cardiac-specific deletion of acetyl CoA carboxylase 2 prevents metabolic remodeling during pressure-overload hypertrophy. *Circ. Res.* **111**: 728–738.

Krissinel E, Henrick K. 2007. Inference of macromolecular assemblies from crystalline state. *J. Mol. Biol.* **372**: 774–797.

LaFave LT, Augustin LB, Mariash CN. 2006. S14: insights from knockout mice. *Endocrinology* **147**: 4044–4047.

Lopaschuk GD, Ussher JR, Folmes CD, Jaswal JS, Stanley WC. 2010. Myocardial fatty acid metabolism in health and disease. *Physiol. Rev.* **90**: 207–258.

Luckow VA, Lee SC, Barry GF, Olins PO. 1993. Efficient generation of infectious recombinant baculoviruses by site-specific transposon-mediated insertion of foreign genes into a baculovirus genome propagated in Escherichia coli. *J. Virol.* **67**: 4566–4579.

Ma L, Tsatsos NG, Towle HC. 2005. Direct role of ChREBP.Mlx in regulating hepatic glucose-responsive genes. *J. Biol. Chem.* **280**: 12019–12027.

Maeda S, Kawai T, Obinata M, Fujiwara H, Horiuchi T, Saeki Y, Sato Y, Furusawa M. 1985. Production of human α-interferon in silkworm using a baculovirus vector. *Nature* **315**: 592–594.

Mater MK, Thelen AP, Pan DA, Jump DB. 1999. Sterol response element-binding protein 1c (SREBP1c) is involved in the polyunsaturated fatty acid suppression of hepatic S14 gene transcription. *J. Biol. Chem.* **274**: 32725–32732.

Motohashi T, Shimojima T, Fukagawa T, Maenaka K, Park EY. 2005. Efficient large-scale protein production of larvae and pupae of silkworm by *Bombyx mori* nuclear polyhedrosis virus bacmid system. *Biochem. Biophys. Res. Commun.* **326**: 564–569.

Muoio DM, Newgard CB. 2006. Obesity-related derangements in metabolic regulation. *Annu. Rev. Biochem.* **75**: 367–401.

Naldini L, Blomer U, Gallay P, Ory D, Mulligan R, Gage FH, Verma IM, Trono D. 1996. In vivo gene delivery and stable transduction of nondividing cells by a lentiviral vector. *Science* **272**: 263–267.

Ogata M, Nakajima M, Kato T, Obara T, Yagi H, Kato K, Usui T, Park EY. 2009. Synthesis of sialoglycopolypeptide for potentially blocking influenza virus infection using a rat a2,6-sialyltransferase expressed in BmNPV bacmid-injected silkworm larvae. *BMC Biotechnol.* **9**: 54.

Olson TM, Alekseev AE, Liu XK, Park S, Zingman LV, Bienengraeber M, Sattiraju S, Ballew JD, Jahangir A, Terzic A. 2006. Kv1.5 channelopathy due to *KCNA5* loss-of-function mutation causes human atrial fibrillation. *Hum. Mol. Genet.* **15**: 2185–2191.

Park S, Terzic A. 2010. Quaternary structure of K_{ATP} channel SUR2A nucleotide binding domains resolved by synchrotron radiation X-ray scattering. *J. Struct. Biol.* **169**: 243–251.

Park EY, Kageshima A, Kwon MS, Kato T. 2007. Enhanced production of secretory b1,3-*N*-acetylglucosaminyltransferase 2 fusion protein into hemolymph of *Bombyx mori* larvae using recombinant BmNPV bacmid integrated signal sequence. *J. Biotechnol.* **129**: 681–688.

Park S, Lim BB, Perez-Terzic C, Mer G, Terzic A. 2008. Interaction of asymmetric *ABCC9*-encoded nucleotide binding domains determines K_{ATP} channel SUR2A catalytic activity. *J. Proteome Res.* **7**: 1721–1728.

Park EY, Ishikiriyama M, Nishina T, Kato T, Yagi H, Kato K, Ueda H. 2009. Human IgG1 expression in silkworm larval hemolymph using BmNPV bacmids and its *N*-linked glycan structure. *J. Biotechnol.* **139**: 108–114.

Reyes S, Park S, Johnson BD, Terzic A, Olson TM. 2009. K_{ATP} channel Kir6.2 E23K variant overrepresented in human heart failure is associated with impaired exercise stress response. *Human Genet* **126**: 779–89.

Reyes S, Park S, Terzic A, Alekseev AE. 2010. K_{ATP} channels process nucleotide signals in muscle thermogenic response. *Crit. Rev. Biochem. Mol. Biol.* **45**: 506–519.

Saggerson D. 2008. Malonyl-CoA, a key signaling molecule in mammalian cells. *Ann. Rev. Nutr.* **28**: 253–272.

Sahin E, Roberts CJ. 2012. Size-exclusion chromatography with multi-angle light scattering for elucidating protein aggregation mechanisms. *Methods Mol. Biol.* **899**: 403–423.

Sakuma T, Barry MA, Ikeda Y. 2012. Lentiviral vectors: basic to translational. *Biochem. J.* **443**: 603–618.

Seelig S, Liaw C, Towle HC, Oppenheimer JH. 1981. Thyroid hormone attenuates and augments hepatic gene expression at a pretranslational level. *Proc. Natl. Acad. Sci. U. S. A.* **78**: 4733–4737.

Shen Y, Volrath SL, Weatherly SC, Elich TD, Tong L. 2004. A mechanism for the potent inhibition of eukaryotic acetyl-coenzyme A carboxylase by soraphen A, a macrocyclic polyketide natural product. *Mol. Cell* **16**: 881–891.

Striegel AM, Brewer AK. 2012. Hydrodynamic chromatography. *Annu. Rev. Anal. Chem. (Palo Alto Calif.)* **5**: 15–34.

Tamura T, Thibert C, Royer C, Kanda T, Abraham E, Kamba M, Komoto N, Thomas JL, Mauchamp B, Chavancy G, Shirk P, Fraser M, Prudhomme JC, Couble P. 2000. Germline transformation of the silkworm Bombyx mori L. using a piggyBac transposon-derived vector. *Nat. Biotechnol.* **18**: 81–84.

Teule F, Miao YG, Sohn BH, Kim YS, Hull JJ, Fraser MJ, Jr., Lewis RV, Jarvis DL. 2012. Silkworms transformed with chimeric silkworm/spider silk genes spin composite silk fibers with improved mechanical properties. *Proc. Natl. Acad. Sci. U. S. A.* **109**: 923–928.

Thampy KG, Wakil SJ. 1988. Regulation of acetyl-coenzyme A carboxylase. I. Purification and properties of two forms of acetyl-coenzyme A carboxylase from rat liver. *J. Biol. Chem.* **263**: 6447–6453.

Tomita M, Munetsuna H, Sato T, Adachi T, Hino R, Hayashi M, Shimizu K, Nakamura N, Tamura T, Yoshizato K. 2003. Transgenic silkworms produce recombinant human type III procollagen in cocoons. *Nat. Biotechnol.* **21**: 52–56.

Tong L. 2005. Acetyl-coenzyme A carboxylase: crucial metabolic enzyme and attractive target for drug discovery. *Cell. Mol. Life Sci.* **62**: 1784–1803.

Tong L. 2013. Structure and function of biotin-dependent carboxylases. *Cell. Mol. Life Sci.* **70**: 863–891.

Vandenborre G, Smagghe G, Ghesquiere B, Menschaert G, Nagender Rao R, Gevaert K, Van Damme EJ. 2011. Diversity in protein glycosylation among insect species. *PloS one.* **6**: e16682.

Wakil SJ, Abu-Elheiga LA. 2009. Fatty acid metabolism: target for metabolic syndrome. *J. Lipid Res.* **50**(Suppl): S138–143.

Wittig I, Braun HP, Schagger H. 2006. Blue native PAGE. *Nat. Protoc.* **1**: 418–428.

Wolfgang MJ, Lane MD. 2011. Hypothalamic malonyl-CoA and CPT1c in the treatment of obesity. *FEBS J.* **278**: 552–558.

Zufferey R, Nagy D, Mandel RJ, Naldini L, Trono D. 1997. Multiply attenuated lentiviral vector achieves efficient gene delivery in vivo. *Nat. Biotechnol.* **15**: 871–875.

SUPPORTING INFORMATION

Additional supporting information may be found in the online version of this article at the publisher's web site.